

Development of a Torque Vectoring System in Hybrid 4WD Vehicles to Improve Vehicle Safety and Agility

Giseo Park, and Seibum B. Choi, *Member, IEEE*

Abstract— In this paper, a new method for vehicle torque vectoring (TV) with the difference in torques between the left and right sides is introduced. This chassis control system can help the vehicle follow the driver’s intended line without vehicle deceleration. Targeting a hybrid four wheel drive (4WD) vehicle with an active differential in rear axle and in-wheel motors (IWMs) in front axle, a TV system based on a vehicle bicycle model is developed. Especially, a new yaw rate reference smoothly varying between safety mode and sport mode aims to enhance both cornering safety and agility. To properly combine these two modes, a weighting factor based on steering command is designed. Also, to track the reference accurately, an integral sliding mode controller (SMC) is introduced in this paper, which has the advantage of reducing yaw rate error during steady state cornering. Lastly, a torque distribution method based on modeling of both active differential and IWM is developed to generate the correct yaw moment. Also, it reflects the actuator characteristics, such as response time, torque capacity, and torque direction. The performance of the proposed TV system is evaluated using a vehicle dynamic software, and a comparative study is also conducted.

I. INTRODUCTION

A vehicle torque vectoring (TV) system, which varies torque to each wheel independently, aims at both improved traction and handling performances [1]. In keeping with consumers’ growing demand for high-performance vehicles, this TV system is considered a beneficial chassis control system for the vehicle cornering response [2]. In some previous papers, state-of-the-arts of TV system were proposed.

In [1], TV system with the optimal wheel torque distribution was proposed. However, the optimization procedure in this logic has to be implemented offline only. In [2], integration of yaw rate and sideslip controllers based on phase-plane analysis was suggested to allow the sustained high values of sideslip angle. Also, TV system with constrained optimization (CA) of tire force was found in [3]. However, feedback errors from the estimated sideslip angle may cause robustness issues in these algorithms. Integral sliding mode controller (SMC) to be robust to tire model uncertainty was developed in [4] and also, optimal TV system based on linear matrix inequality (LMI) was introduced in [5], respectively. But, the computational burden problem may arise in these algorithms. Considering the limitations of previous studies, the goal of this paper is the development of a practical TV system.

Most commercialized TV systems are based on the active differential connected to the mechanical driveline devices. However, to overcome some limitations of active differential related to response time, maximum allowable yaw moment

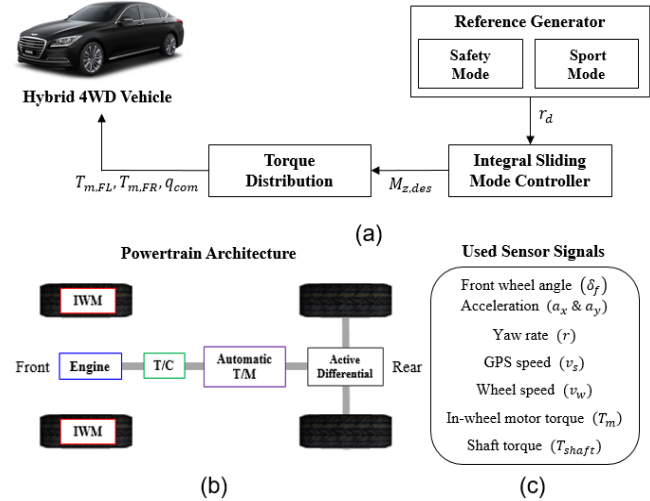


Figure 1. Block diagrams of overall algorithm.

and environmental friendliness [6], the proposed TV system is applied to the hybrid four wheel drive (4WD) system that two in-wheel motors (IWMs) of the front wheels coexists with the active differential in the rear axle (front-engine, rear-drive layout). A block diagram of the overall algorithm is illustrated in Fig. 1. The major differences distinguishing the suggested algorithm from the previous researches are as follows. First, the desired yaw rate from the reference generator leads to a sport mode increasing rear tire slip angle during the specific situation. Therefore, the driver’s fun-to-drive can be attained qualitatively while improving the agility of the vehicle in a quantitative aspect. Second, a practical torque distribution method reflects the characteristics of both active differential and IWM in terms of response time, torque capacity, and torque direction.

This paper is comprised of five sections. Section II presents the vehicle model and the reference generator. In Section III, both the integral SMC combined with an integral feedback term and the torque distribution algorithm are introduced. In Section VI, simulation study is conducted to validate the proposed TV system. Finally, in Section V, the conclusion is presented.

II. REFERENCE GENERATOR

As mentioned above, the goal of TV system is to improve both vehicle safety and agility according to cornering situations. By combining the safety mode reference $r_{d,safety}$ with the sport mode reference $r_{d,sport}$, a new reference model

G. Park and S. B. Choi are with the Department of Mechanical Engineering, Korea Advanced Institute of Science and Technology (KAIST), Daejeon 34141, Korea (e-mail: giseo123@kaist.ac.kr; sbchoi@kaist.ac.kr).

can be generated. Here, $r_{d,sport}$ is inspired by drifting, which is the high sideslip maneuver undertaken by skilled drivers [7]. As this drifting aims at tire force saturation of the rear wheels, the sport mode increases the lateral tire force of the rear wheels to a certain level. As shown in Fig. 2, both safety and sport modes are visualized in detail. As the rear tire slip angles increases in the sport mode, the sideslip angle also increases, which makes the vehicle moves sideways to some extent. The slip angle difference between the front and the rear wheels becomes smaller in comparison with the safety mode, so that the understeering tendency is certainly reduced.

A. Vehicle Bicycle Model

In this section, the vehicle bicycle model considering the vehicle dynamics on the only yaw plane is utilized. This bicycle model combines the tire forces of both wheels at the center line [8]. Since the wheels are assumed to be located at the center line, this model can be more easily utilized for the development of a lateral dynamic controller. The moment and lateral force balance equations in this bicycle model are expressed as follows:

$$I_z \dot{r} = F_{yf} l_f - F_{yr} l_r \quad (1)$$

$$m v_x (\dot{\beta} + r) = F_{yf} + F_{yr} \quad (2)$$

Here, I_z is the yaw moment of inertia of a vehicle; β the vehicle sideslip angle; v_x the longitudinal velocity; m the total mass of a vehicle; and r the vehicle yaw rate. Also, l_f and l_r are the CG-front and CG-rear axle distances, respectively. The lateral tire forces lumped at the front and rear axles can be derived as

$$F_{yf} = (m l_r a_y + I_z \dot{r}) / (l_f + l_r) \quad (3)$$

$$F_{yr} = (m l_f a_y - I_z \dot{r}) / (l_f + l_r) \quad (4)$$

where a_y is the lateral acceleration at CG. The wheel slip angles of the front and the rear axles are expressed as

$$\alpha_f = \beta + l_f r / v_x - \delta_f \quad (5)$$

$$\alpha_r = \beta - l_r r / v_x \quad (6)$$

Here, δ_f is the front steering angle.

B. Safety Mode

Generally, the steady state of the bicycle model is considered the control reference (i.e., $\dot{r} = 0$ and $\dot{\beta} = 0$ in (1) and (2)). Assuming that the lateral tire force is linearly proportional to the wheel slip angle (i.e., $F_{yf} = -C_f \alpha_f$ and $F_{yr} = -C_r \alpha_r$), The desired yaw rate for safety mode reflecting both vehicle speed and driver's steering command can be obtained as follows [4, 8]:

$$r_{d,safety} = \frac{v_x}{l_f + l_r + \frac{m(l_r C_r - l_f C_f)}{2(l_f + l_r) C_f C_r} v_x^2} \delta_f \quad (7)$$

Also, C_f and C_r mean the cornering stiffness of the front and rear axles, respectively.

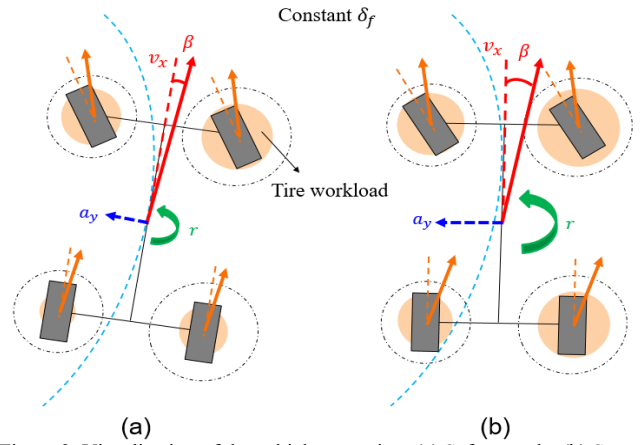


Figure 2. Visualization of the vehicle cornering. (a) Safety mode. (b) Sport mode.

C. Sport Mode

As seen in Fig. 2, in the case of same longitudinal speed and steering command, what has to be noted is that the tire workload of each wheel increases enough to get closer to the friction limit in the sport mode. Then, the sport mode yields both the higher yaw gain and the maximum of lateral acceleration than the safety mode. To implement this mode, firstly, the saturation point of the rear tire $\alpha_{r,sat}$ where the tire contact patch reaches to the friction limit is introduced as follows (from the lateral brushed tire model [7]):

$$\alpha_{r,sat} = \tan^{-1}(3\mu F_{zr} / C_r) \quad (8)$$

where

$$F_{zr} = (m g l_f + m h a_x) / (l_f + l_r) \quad (9)$$

Here, h is the height of CG; a_x the longitudinal acceleration at CG; and μ the tire-road friction coefficient (TRFC): TRFC estimation algorithm is introduced in [9]. To make that α_r tracks $\alpha_{r,d}$ ($= \eta \alpha_{r,sat}$), the desired yaw rate of the sport mode (from (6)) can be derived as

$$r_{d,sport} = (\beta_d - \alpha_{r,d}) v_x / l_r \quad (9)$$

where the desired sideslip angle is as follows [10]:

$$\beta_d = \eta \frac{l_r - \frac{m l_f v_x^2}{L C_r}}{L + \frac{m(l_r C_r - l_f C_f)}{L C_f C_r} v_x^2} \delta_f$$

The factor η ($0 \leq \eta \leq 1$) is determined according to vehicle specifications and system features. In [11, 12], the integrated observer using in-vehicle sensors to estimate the tire cornering stiffness was suggested.

D. Weighting Factor Design

The sport mode has to be operated in a situation when the surrounding environment is not restricted enough to enjoy fun-to-drive. With the weighting factor K between $r_{d,safety}$ and $r_{d,sport}$, the final reference is derived as follows:

$$r_d = (1 - K) r_{d,safety} + K r_{d,sport} \quad (10)$$

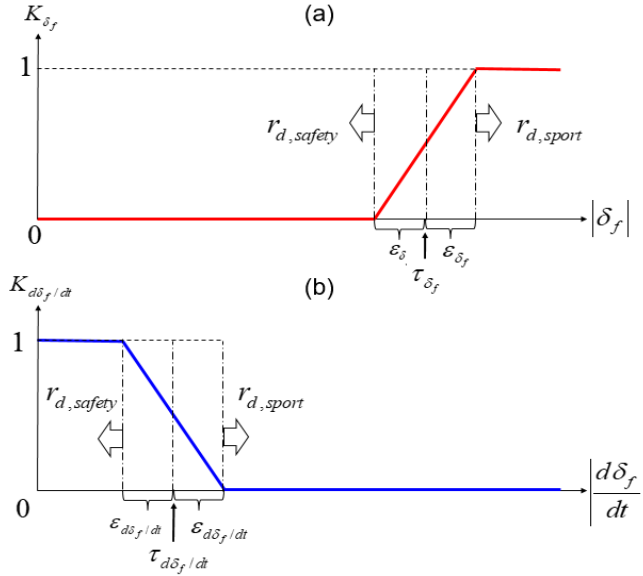


Figure 3. Visualization of sub-weighting factors. (a) K_{δ_f} . (b) $K_{d\delta_f/dt}$.

To determine the proper weighting factor in real time, the characteristics of the driver's steering commands and road conditions are analyzed. The sub-weighting factors are defined in (11), which are constructed in the form of a saturated function that varies between 0 and 1.

$$\begin{aligned} K_\mu &= \text{sat}[(\mu - \tau_\mu + \varepsilon_\mu) / (2\varepsilon_\mu)] \\ K_{\delta_f} &= \text{sat}[(|\delta_f| - \tau_{\delta_f} + \varepsilon_{\delta_f}) / (2\varepsilon_{\delta_f})] \\ K_{d\delta_f/dt} &= 1 - \text{sat}[(|d\delta_f/dt| - \tau_{d\delta_f/dt} + \varepsilon_{d\delta_f/dt}) / (2\varepsilon_{d\delta_f/dt})] \end{aligned} \quad (11)$$

Here, τ and ε are the positive tuning parameters in saturation functions. Fig. 3 presents how the sub-weighting factors K_{δ_f} and $K_{d\delta_f/dt}$ are obtained as a function of the absolute values of δ_f and $d\delta_f/dt$, respectively. It implies that the sport mode is implemented during specific steering commands, i.e. both large steering angle and small steering rate at the same time. Also, the other factor in (11), K_μ denotes that this mode has to be activated on a high- μ surface, where the road condition is suitable for more aggressive driving. By multiplying these sub-weighting factors, the final weighting factor is derived as follows:

$$K = K_\mu K_{\delta_f} K_{d\delta_f/dt}. \quad (12)$$

As a result, K provides a smoothly varying weighting sum, which reduces both discontinuity of controller reference and riding discomfort between $r_{d,safety}$ and $r_{d,sport}$. Then, cornering situations when the sport mode is not activated are as follows.

- 1) Driving on a low- μ surface, e.g. $\mu \leq 0.5$.
- 2) Mild steering commands with small δ_f .
- 3) Urgent driving situations with rapid change of the steering angle, e.g. lane change and collision avoidance.

III. INTEGRAL SLIDING MODE CONTROLLER

A. Controller Design

To track the yaw rate reference in (10), the integral SMC is proposed in this section. Firstly, consider that the yaw moment M_z is added to (1):

$$\dot{r} = (l_f F_{yf} - l_r F_{yr} + M_z) / I_z. \quad (13)$$

The tracking error e is defined as

$$e = r - r_d. \quad (14)$$

To design the control input, let \dot{e} be the sum of the saturation function $\text{sat}(\cdot)$ and the integral term of e : $\text{sat}(\cdot)$, used instead of the sign function $\text{sgn}(\cdot)$, prevents SMC chattering problems.

$$\dot{e} = -\lambda_p \text{sat}(e / \phi) - \lambda_I \int_0^t e dt \quad (15)$$

where

$$\text{sat}(e / \phi) = \begin{cases} 1 & (\phi < e) \\ e / \phi & (-\phi \leq e \leq \phi) \\ -1 & (e < -\phi) \end{cases}$$

Here, λ_p and λ_I are the positive proportional (P) and integral (I) gains, respectively. Also, ϕ denotes the small positive value. Then, error dynamics can be written as

$$\dot{r} - \dot{r}_d + \lambda_p \text{sat}(e / \phi) + \lambda_I \int_0^t e dt = 0. \quad (16)$$

By Substituting (13) into (16), the control input is designed as

$$M_{z,des} = -l_f F_{yf} + l_r F_{yr} + I_z \dot{r}_d - \lambda_p I_z \text{sat}(e / \phi) - \lambda_I I_z \int_0^t e dt. \quad (17)$$

The integral term takes the role of reducing the residual error, and especially, it can effectively eliminate the steady state error of the yaw rate during the sport mode. To prove stability, Lyapunov function candidate V , which is lower bounded and positive definite ($V > 0$), is defined as follows:

$$V = e^2 / 2 + \lambda_I (\int_0^t e dt)^2 / 2. \quad (18)$$

Then, the time derivative of V is derived as

$$\dot{V} = e\dot{e} + \lambda_I e \int_0^t e dt. \quad (19)$$

Substituting (15) into (19) yields

$$\dot{V} = -\lambda_p e \cdot \text{sat}(e / \phi) \quad (20)$$

which is negative semidefinite ($\dot{V} \leq 0$). From (18) and (20), it is proven by Lasalle's theorem that the origin is asymptotically stable, i.e., tracking error e converges to 0 [13].

B. Torque Distribution – Active Differential

To generate a yaw moment corresponding to $M_{z,des}$ in (17), a method to distribute torque to each wheel is proposed. The torque to be transmitted to the active differential in the rear axle is obtained in advance. Then, insufficient yaw moment production is compensated by IWM torque in the front wheels. The active differential is available to transfer the torque to the inner or outer wheels in various torque ratios. When TV system is deactivated, the active differential transmits the equal torque $T_{shaft}/2$ to the left and the right wheels, like an open differential. Contrary, the left and right torques are split

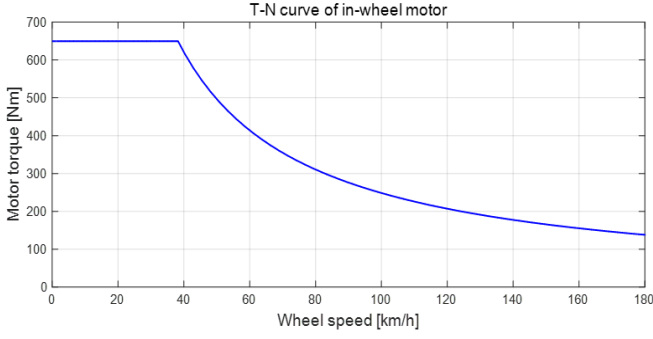


Figure 4. T-N curve of in-wheel motor.

TABLE I. VEHICLE SPECIFICATIONS

Parameter	Quantity	Value
m	Total vehicle mass	1530 kg
l_f	CG-front axle distance	1.11 m
l_r	CG-rear axle distance	1.67 m
I_z	Yaw moment of inertia	2315 kg · m ²
R_e	Effective tire radius	0.325 m
h	Height of CG	0.52 m
t	Track width	1.55 m
T_{cl}	Maximum clutch torque	400 Nm
τ_c	Time constant of active differential	0.25 sec
C_f	Tire cornering stiffness of front axle	117000 N/rad
C_r	Tire cornering stiffness of rear axle	86800 N/rad

with TV system activation. In the case that the clutch with a distribution ratio q ($0 \leq q \leq 1$) is engaged, the drive torques transmitted to the left and right wheel are modeled as follows [10]:

$$T_{shaft,RL} = T_{shaft} / 2 - qT_{cl} \quad (21)$$

$$T_{shaft,RR} = T_{shaft} / 2 + qT_{cl} \quad (22)$$

Here, T_{cl} is the maximum clutch torque of active differential. Negative and positive q denotes the engagement of left and right clutches, respectively. This q can be expressed as a first-order transfer function of the clutch input command q_{com} i.e. $q(s) = sat(q_{com}/\phi_q)/(\tau_c s + 1)$. Here, the time constant τ_c can reflect the response time of active differential. Also, ϕ_q is the saturation parameter corresponding to a maximum torque ratio between $T_{shaft,RL}$ and $T_{shaft,RR}$ (e.g. the ratio 3:1 represents $\phi_q = T_{shaft}/(4T_{cl})$). According to $M_{z,des}$, this q_{com} is designed with the threshold M_{z,R_lim} .

$$q_{com} = \begin{cases} -1 & (M_{z,des} < -M_{z,R_lim}) \\ M_{z,des}/M_{z,R_lim} & (-M_{z,R_lim} \leq M_{z,des} \leq M_{z,R_lim}) \\ 1 & (M_{z,R_lim} < M_{z,des}) \end{cases} \quad (23)$$

Finally, assuming that the longitudinal tire force is expressed as $F_x \approx T_d/R_e$, the yaw moment generated in the rear axle is

$$M_{z,R} = t(F_{x,RR} - F_{x,RL})/2 = \frac{tT_{cl}}{R_e(\tau_c s + 1)} sat(q_{com}/\phi_q) \quad (24)$$

where t is the track width; R_e the effective tire radius; and T_d the drive torque of the wheel.

C. Torque Distribution – In-Wheel Motor

The yaw moment generated in the front axle $M_{z,F}$ is equal to $M_{z,des} - M_{z,R}$. Because of the inverse relationship between motor torque and angular speed, the maximum motor torque $T_{m,max}$ can be a function of the angular speed. Then, the actual T-N curve of IWM is shown in Fig. 4. The maximum yaw moment that can be generated by only one IWM torque is

$$M_{z,F_lim} = tT_{m,max} / (2R_e). \quad (25)$$

If a small magnitude of $M_{z,F}$ is required ($|M_{z,F}| \leq M_{z,F_lim}$), it is desired to operate only one IWM torque (a negative motor torque of the other IWM at high velocity may cause excessive regenerative braking and it may lead to deterioration of the durability of IWM). By contrast, in the case of requiring a large magnitude of $M_{z,F}$ ($|M_{z,F}| > M_{z,F_lim}$), it is inevitable to use both IWMs in order to generate a large amount of yaw moment. The accurate yaw moment generation is prioritized over other keys. Based on these findings, the rules of torque distribution of IWMs are proposed as follows.

$$T_{m,FL} = \begin{cases} -R_e M_{z,F} / t & (M_{z,F} < -M_{z,F_lim}) \\ -2R_e M_{z,F} / t & (-M_{z,F_lim} \leq M_{z,F} < 0) \\ 0 & (0 \leq M_{z,F} \leq M_{z,F_lim}) \\ -R_e M_{z,F} / t & (M_{z,F_lim} < M_{z,F}) \end{cases} \quad (26)$$

$$T_{m,FR} = \begin{cases} R_e M_{z,F} / t & (M_{z,F} < -M_{z,F_lim}) \\ 0 & (-M_{z,F_lim} \leq M_{z,F} < 0) \\ 2R_e M_{z,F} / t & (0 \leq M_{z,F} \leq M_{z,F_lim}) \\ R_e M_{z,F} / t & (M_{z,F_lim} < M_{z,F}) \end{cases} \quad (27)$$

IV. SIMULATION STUDY

To evaluate the performance of the proposed TV system, simulation studies are described in this section. The vehicle dynamics solver packages CarSim and MATLAB/Simulink are utilized. The used vehicle model is the E-class sedan with the parameters of an actual luxury sedan (Hyundai Genesis DH), as shown in Table I. This model is driven by the engine power of 200 kW. The tire model of each wheel is set to the Magic Formula tire model. From the following two simulation cases, the effectiveness of the proposed algorithm is evaluated fairly with other control modes. Also, in order to check its practicality, all tuning parameters are set to constant values as follows: $\lambda_p = 10$, $\lambda_l = 2$, $\phi = 1$, $M_{z,R_lim} = 2500$ Nm, $\varepsilon_{\delta_f} = 10$ deg, $\varepsilon_{d\delta_f/dt} = 5$ deg/s, $\tau_{\delta_f} = 40$ deg, $\tau_{d\delta_f/dt} = 10$ deg/s, and the factor η in (23) is 0.5. Then, there are some thresholds for TV system activation: $|a_y| \geq 0.2$ g, $v_x \geq 40$ km/h, and $P_{mc} \leq 2$ MPa [14, 15].

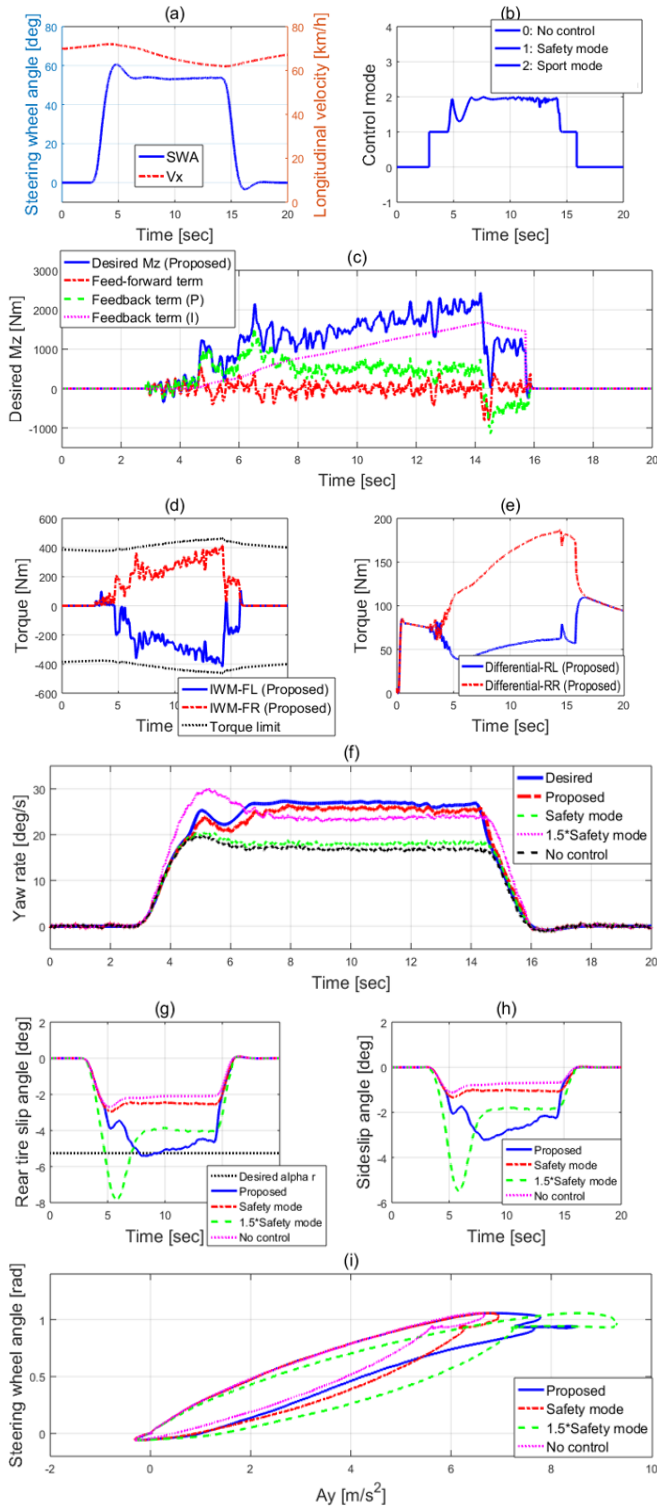


Figure 5. Circle turn test results on a high-mu road surface ($\mu = 1$).

A. Case 1 (Circle Turn Test)

Figure 5 depicts the simulation results on a high-mu road surface ($\mu = 1$). In this case, the circle turn test with a long radius (70 m) is conducted. Also, the driver steps on the acceleration pedal to keep the vehicle longitudinal speed at 70 km/h, as shown in Fig. 5 (a). Along with the desired yaw moment in Fig. 5 (c), some yaw moment terms that make up

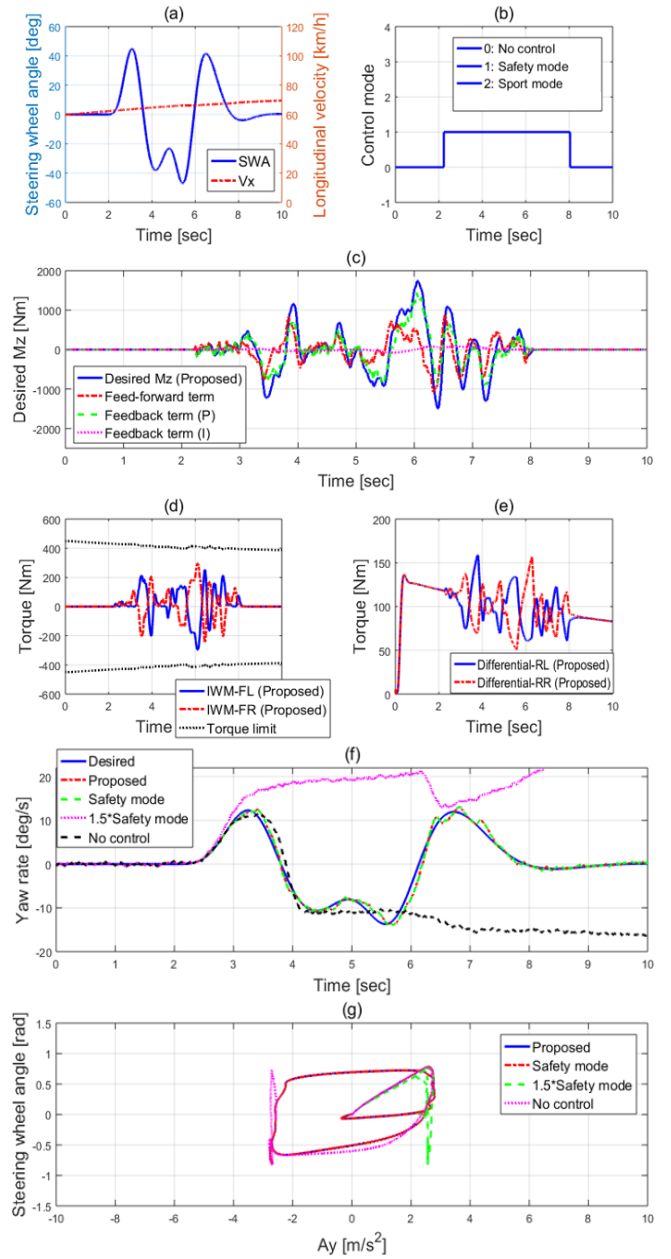


Figure 6. DLC test results on a low-mu road surface ($\mu = 0.3$).

$M_{z,des}$ are shown: the feed-forward term $l_r F_{yr} - l_f F_{yf} + l_z \dot{r}_d$, the proportional and integral terms of feedback error, $-\lambda_p I_z \text{sat}(e/\phi)$ and $-\lambda_I I_z \int_0^t e dt$.

In transient states when the circle turn starts and ends, the feed-forward term makes the actual yaw rate to quickly follow the desired yaw rate. Also, during the steady state with the constant yaw rate, the integral feedback term gradually increases to reduce the steady state error. As the steering angle becomes constant at zero, this term automatically sets to zero.

In Figs. 5 (d) and (e), drive torques in front and rear axles are presented, respectively. The drive torques of the outer wheels become larger than those of the inner wheels. The active differential of real axle yields a smaller amount of yaw moment and slower response time than IWM of the front axle due to the limitation of maximum torque ratio between $T_{shaft,RL}$ and $T_{shaft,RR}$. However, IWM torques appear to be

accompanied by some noise and vibration.

Under the same driver's input, the yaw rate trajectory of the proposed algorithm (to follow r_d in (10)) is illustrated comparing with other modes in Fig. 5 (f): the safety mode aims to follow $r_{d,safety}$ in (7). It is confirmed that the proposed algorithm leads a noticeably larger yaw rate than safety mode and no control mode. If $r_{d,safety}$ of the safety mode is multiplied by 1.5 (1.5*safety mode) to make the yaw rate as large as the proposed algorithm, the unintentional dangerous situation occurs with the overshoot of the rear tire slip angle, as shown in Fig. 5 (g). In contrast, without any overshoot issues, the proposed algorithm increases the rear tire slip angle to near the target value $\alpha_{r,d}(= 0.5\alpha_{r,sat})$. Also, the sideslip angle in Fig. 5 (h) shows similar tendency. Finally, as seen in Fig. 5 (i), the understeer characteristic curve (one of the well-known methods to evaluate the vehicle agility) of the proposed algorithm has lower slope than that of the safety mode: 1.5*safety mode has too excessively low slope. These facts mean that the driver with the proposed algorithm can feel fun-to-drive with higher slip angle, together with the increased vehicle agility.

B. Case 2 (Double Lane Change Test)

In the double lane change (DLC) test, how the proposed algorithm operates in hazardous situations such as the extreme steering maneuver on a low- μ road surface ($\mu = 0.3$). Figure 6 (a) describes the severe steering angle command and slowly increasing longitudinal velocity from 60 km/h. As shown in Fig. 6 (c), $M_{z,des}$ is vigorously changed according to the severe steering angle command. Since there is almost no steady state region in DLC test compared with the circle turn test, the proportion of the integral feedback term is close to zero. In doing so, $M_{z,des}$ induces the actively varying torques in Figs. 6 (d) and (e).

Since the final weighting factor K is zero during this DLC maneuver, the reference of the proposed algorithm r_d is equal to that of the safety mode $r_{d,safety}$. In cases of both 1.5*safety mode and no control mode, the wheels lose tire grip and the vehicle spins out completely, as shown in Figs. 6 (f) and (g).

V. CONCLUSION

In this paper, a new TV system for hybrid 4WD vehicles considers the improvement of both vehicle safety and agility. It consists of three subsystems (reference generator, integral SMC, and torque distribution), all of which are designed differently from previous studies. Especially, the reference generator combining the safety mode with the sport mode actively leads to the rear tire slip increment, so that some ordinary drivers can feel sufficient fun-to-drive just as drifting undertaken by skilled drivers. With the real car parameter-based simulation, high cornering performance of the proposed TV system has been confirmed. The major contributions are summarized as follows.

(1) With the weighting factor between $r_{d,safety}$ and $r_{d,sport}$, TV system provides the smoothly varying reference r_d considering vehicle safety and agility simultaneously.

(2) The integral SMC can effectively reduce the steady state error during the slow change of the steering angle, such as the circle turn.

(3) The torque distribution method is practical with

relatively small computational burden. Also, it reflects the characteristics of both active differential and IWM, such as response time, torque capacity, and torque direction.

In conclusion, the proposed TV system can be a meaningful solution for the cornering performance improvement of hybrid 4WD vehicles.

ACKNOWLEDGMENT

This research was partly supported by the National Research Foundation of Korea(NRF) grant funded by the Korea government(MSIP) (No. 2017R1A2B4004116); the BK21+ program through the NRF funded by the Ministry of Education of Korea; and the Technology Innovation Program or Industrial Strategic Technology Development Program (10084619, Development of Vehicle Shock Absorber (Damper) and Engine Mount Using MR Fluid with Yield Strength of 60kPa) funded by the Ministry of Trade, Industry & Energy (MOTIE, Korea).

REFERENCES

- [1] L. Novellis, A. Sorniotti, and P. Gruber, "Wheel Torque Distribution Criteria for Electric Vehicles With Torque-Vectoring Differentials," *IEEE Trans. Veh. Technol.*, vol. 63, pp. 1593-1602, 2014.
- [2] Q. Lu, P. Gentile, A. Tota, A. Sorniotti, P. Gruber, F. Costamagna, and J. Smet, "Enhancing vehicle cornering limit through sideslip and yaw rate control," *Mech. Sys. And Sig. Process.*, vol. 75, pp. 455-472, 2016.
- [3] D. Kasinathan, A. Kasaiezadeh, A. Wong, A. Khajepour, S. Che, and B. Litkouhi, "An Optimal Torque Vectoring Control for Vehicle Applications via Real-Time Constraints," *IEEE Trans. Veh. Technol.*, vol. 65, pp. 4368-4378, 2016.
- [4] T. Goggia, A. Sorniotti, L. Novellis, A. Ferrara, P. Gruber, J. Theunissen, D. Steenbeke, B. Knauder, and J. Zehetner, "Integral Sliding Mode for the Torque-Vectoring Control of Fully Electric Vehicles: Theoretical Design and Experimental Assessment," *IEEE Trans. Veh. Technol.*, vol. 64, pp. 1701-1715, 2015.
- [5] S. Fallah, A. Khajepour, B. Fidan, S. Chen, and B. Litkouhi, "Vehicle Optimal Torque Vectoring Using State-Derivative Feedback and Linear Matrix Inequality," *IEEE Trans. Veh. Technol.*, vol. 62, pp. 1540-1552, 2013.
- [6] B. Ren, H. Chen, H. Zhao, and L. Yuan, "MPC-based yaw stability control in in-wheel-motored EV via active front steering and motor torque distribution," *Mechatronics*, vol. 38, pp. 103-114, 2016.
- [7] C. Coser, R. Hindiyeh, and J. Gerdes, "Analysis and control of high sideslip manoeuvres," *Vehi. Sys. Dyn.*, vol. 48, pp. 317-336, 2010.
- [8] G. Park, and S. Choi, "Optimal Brake Distribution for Electronic Stability Control Using Weighted Least Square Allocation Method," in *2016 16th Int. Conf. Con. Auto. Sys.*, pp. 1420-1425.
- [9] K. Han, E. Lee, M. Choi, and S. Choi, "Adaptive Scheme for the Real-Time Estimation of Tire-Road Friction Coefficient and Vehicle Velocity," *IEEE Trans. Mechatronics*, vol. 22, pp. 1508-1518, 2017.
- [10] R. Rajamani, *Vehicle Dynamics and control*: New York, NY: Springer-Verlag, 2006.
- [11] G. Park, S. Choi, D. Hyun, and J. Lee, "Integrated Observer Approach Using In-vehicle Sensors and GPS for Vehicle State Estimation," *Mechatronics*, vol. 50, pp.134-147, 2018.
- [12] P. A. Ioannou and J. Sun, *Robust adaptive control*: North Chelmsford, M: Courier Corporation, 2012.
- [13] H. K. Khalil and J. Grizzle, *Nonlinear systems* vol. 3: Prentice hall New Jersey, 1996.
- [14] G. Park, Y. Hwang, and S. Choi, "Vehicle positioning based on velocity and heading angle observer using low-cost sensor fusion," *J. Dyn. Sys., Meas., Control*, vol. 139, no. 12, pp. 121008-1~13, 2017.
- [15] K. Han, M. Choi, and S. Choi, "Estimation of Tire Cornering Stiffness as a Road Surface Classification Indicator Using Understeering Characteristics," *IEEE Trans. Veh. Technol.*, vol. 67, no. 8. pp. 6851-6860, 2018.